Mitigation of Low-Frequency Oscillations via Oscillation-Critical Nodes Targeting in Grid-Forming Multi-Converter Systems

Feng Tan, Ruohan Leng, Liangxiao Luo, Ruipeng Guo, and Huanhai Xin

***Abstract*—With the development of power electronics technology, grid-forming (GFM) converters enhance the supporting capacity of power systems through the ability to actively establish voltage and frequency. GFM converters are being deployed in large-scale power grids with high renewable energy penetration and low inertia, showing a trend toward large-scale deployment. However, the strong dynamic interaction among multiple GFM converters can easily induce low-frequency oscillations (LFOs), posing a challenge to the small-signal stability of the system. This paper proposes an LFO mitigation strategy based on participation factors of an extended admittance matrix, which enables the accurate identification of only a few oscillation-critical nodes (OCNs) that are most prone to inducing LFOs. The proposed method requires only the largest eigenpair of the extended admittance matrix, thereby achieving a significantly lower computational complexity. By applying targeted control parameter and structure adjustments to GFM converters at these OCNs or switching their operating mode to grid-following (GFL) mode, LFOs can be effectively mitigated with minimal control intervention. Finally, simulation case studies validate the effectiveness of the proposed strategy.**

***Index Terms*—Grid-forming converter, grid-following converter, low-frequency oscillations, small-signal stability.**

I. Introduction

With the large-scale integration of renewable energy, high-voltage direct-current transmission, and other emerging power technologies, power electronic converters have been widely applied in modern power systems. Currently, most converters adopt grid-following (GFL) control strategies, achieving synchronization with the grid through phase-locked loops (PLL) and controlling active and reactive power [1]. However, due to the current source characteristics of GFL converters, their large-scale integration may weaken the ability of the system to support voltage and frequency, thereby affecting the stable operation of the grid. Additionally, in weak-grid environments, GFL converters are prone to sub/super synchronous oscillations driven by the PLL [2], [3].

The deployment of grid-forming (GFM) converters in power systems is considered one of the most effective solutions to the aforementioned problems. GFM converters possess the capability of actively establishing voltage and providing frequency support across multiple time scales, which can effectively enhance the (small-signal) stability of nearby GFL converters [4]. With these advantages, GFM converters are expected to be widely applied in future power systems [5].

However, as the number of GFM converters increases, stability issues arising from multi-converter interactions have become increasingly prominent. This issue has already been observed in practical power systems. For example, in April 2023, the power grid of Kauai Island, Hawaii, experienced approximately 1 Hz low-frequency oscillations (LFOs) induced by the interaction among multiple GFM converters, which had a noticeable impact on the system stability [6].

To enhance the stability of an individual GFM converter, various control strategies have been proposed in existing research. Reference [7] proposed a full-state feedback control strategy to address the coupling issue in the GFM converter. Reference [8] improved the output impedance of the GFM converter through virtual impedance control. These strategies can improve the stability of an individual GFM converter, but they do not consider the interactions among multi-converters. If such control loops are widely deployed in grid-forming multi-converter systems (GFMMSs), it will significantly increase the difficulty of parameter tuning.

For GFMMSs, scholars have also conducted different studies. Reference [9] uses a simulated annealing particle swarm optimization algorithm to adjust the virtual inertia and damping of all GFM converters to mitigate active power oscillations. However, this strategy requires simultaneous adjustments to a large number of parameters, leading to large computational complexity. Reference [10] conducted a stability analysis of the GFMMSs based on the extended passivity theory, but the network topology it relies on is relatively simple and difficult to directly extend to more complex systems.

Therefore, this paper focuses on LFOs in GFMMSs and proposes a mitigation strategy based on participation factors of an extended admittance matrix. From a matrix-theoretic perspective, the paper analytically demonstrates that only a few oscillation-critical nodes (OCNs) that are most prone to inducing LFOs exist in GFMMSs. The identification of OCNs requires only the largest eigenpair of the extended admittance matrix, thereby achieving a significantly lower computational complexity. Based on this identification, LFOs can be effectively mitigated with minimal control intervention by applying targeted control parameter and structure adjustments to the GFM converters at these OCNs, or by switching

This work is supported in part by Smart Grid-National Science and Technology Major Project (2025ZD0804900).

Feng Tan and Liangxiao Luo are with the Polytechnic Institute of Zhejiang University, Hangzhou 310027, China. (Emails: {tanfeng, luolx}@zju.edu.cn), Ruohan Leng, Ruipeng Guo, and Huanhai Xin are with the College of Electrical Engineering, Zhejiang University, Hangzhou 310027, China. (Emails: {lengruohan, eegrp, xinhh}@zju.edu.cn).

979-8-3315-8138-1

their operating mode to GFL.

Accordingly, this paper first establishes the small-signal model of the GFMMSs and, based on perturbation theory, decouples the GFMMSs to obtain the GFM weakest subsystem. Then, the participation factors are employed to identify the OCNs in GFMMSs and implement LFO mitigation. Finally, simulations carried out in MATLAB/Simulink verify the effectiveness of the proposed strategy.

II. Equivalent homogeneous system of GFMMSs

In this section, we first establish the small-signal model of the GFMMSs and, based on perturbation theory, construct an equivalent homogeneous system. Based on this formulation, we then decouple the GFMMSs to obtain its weakest subsystem, which forms the basis for identifying the OCNs.

A. Small-Signal Model of the GFMMSs

We first establish the small-signal model of the GFMMSs in the frequency domain. Taking the GFMMSs shown in Fig. 1 as an example, the systems consist of n renewable plants operating under GFM control. Without loss of generality, each GFM adopts the virtual synchronous generator (VSG) control strategy.

The small-signal model of the i-th converter in the frequency domain is expressed as

$$-\begin{bmatrix}\Delta I_{x,i}\\ \Delta I_{y,i}\end{bmatrix} = S_{\mathrm{B}i}\mathbf{Y}_{\mathrm{C},i}(s)\begin{bmatrix}\Delta U_{x,i}\\ \Delta U_{y,i}\end{bmatrix} \tag{1}$$

where, $\mathbf{Y}_{\mathrm{C},i}(s)$ is a 2×2 transfer function matrix, representing the admittance model of the GFM converter, used to describe the converter's dynamic characteristics, with detailed derivations provided in [5]; $[\Delta I_{x,i}, \Delta I_{y,i}]^T$ and $[\Delta U_{x,i}, \Delta U_{y,i}]^T$ are the current and voltage disturbances output by the i-th converter in the xy coordinate systems; $S_{\mathrm{B}i}$ is the per-unit capacity rating of the i-th converter.

The model of the systems extending from a single-converter system to a multi-converter systems is expressed as

$$-\begin{bmatrix}\Delta I_{x,1}\\ \Delta I_{y,1}\\ \vdots \\ \Delta I_{x,n}\\ \Delta I_{y,n}\end{bmatrix} = (\boldsymbol{S}_{\mathrm{B}}\otimes I_2)\mathbf{Y}_{\mathrm{C}}^{N}(s)\begin{bmatrix}\Delta U_{x,1}\\ \Delta U_{y,1}\\ \vdots \\ \Delta U_{x,n}\\ \Delta U_{y,n}\end{bmatrix} \tag{2}$$

where $\boldsymbol{S}_{\mathrm{B}} = \mathrm{diag}\{S_{\mathrm{B}1}, \ldots, S_{\mathrm{B}n}\} \in \mathbb{R}^{n\times n}$ is a diagonal matrix composed of the per-unit capacity ratings of n GFM converters; I_2 is a 2×2 identity matrix; $\otimes$ denotes the Kronecker product; $\mathbf{Y}_{\mathrm{C}}^{N}(s)$ is the block-diagonal transfer function matrix of dimension $2n\times 2n$, extended from $\mathbf{Y}_{\mathrm{C},i}(s)$, and can be expressed as

$$\mathbf{Y}_{\mathrm{C}}^{N}(s) = \begin{bmatrix}\mathbf{Y}_{\mathrm{C},1}(s) & & & \\ & \mathbf{Y}_{\mathrm{C},2}(s) & & \\ & & \ddots & \\ & & & \mathbf{Y}_{\mathrm{C},n}(s)\end{bmatrix} \tag{3}$$

Next, the small-signal model of the network-side admittance in the frequency domain is expressed as

$$\begin{bmatrix}\Delta I_{x,1}\\ \Delta I_{y,1}\\ \vdots \\ \Delta I_{x,n}\\ \Delta I_{y,n}\end{bmatrix} = \mathbf{Y}_{\mathrm{grid}}(s)\begin{bmatrix}\Delta U_{x,1}\\ \Delta U_{y,1}\\ \vdots \\ \Delta U_{x,n}\\ \Delta U_{y,n}\end{bmatrix} \tag{4}$$

$$\begin{aligned}\mathbf{Y}_{\mathrm{grid}}(s) &= \begin{bmatrix}\mathbf{Y}_{\mathrm{g}1}(s) & \mathbf{Y}_{\mathrm{g}2}(s)\\ \mathbf{Y}_{\mathrm{g}3}(s) & \mathbf{Y}_{\mathrm{g}4}(s)\end{bmatrix}\\ &= \boldsymbol{B}_{\mathrm{red}}\otimes\gamma(s) = \begin{bmatrix}\boldsymbol{B}_{nn} & \boldsymbol{B}_{nm}\\ \boldsymbol{B}_{mn} & \boldsymbol{B}_{mm}\end{bmatrix}\otimes\gamma(s)\end{aligned} \tag{5}$$

$$\boldsymbol{\gamma}(s) = \begin{bmatrix}\dfrac{s}{\omega_0}+\sigma & -1\\ 1 & \dfrac{s}{\omega_0}+\sigma\end{bmatrix}^{-1} \tag{6}$$

where $\mathbf{Y}_{\mathrm{grid}}(s)$ represents the transfer function matrix of the network; $\mathbf{Y}_{\mathrm{g}1}(s), \mathbf{Y}_{\mathrm{g}2}(s), \mathbf{Y}_{\mathrm{g}3}(s)$ and $\mathbf{Y}_{\mathrm{g}4}(s)$ are the four blocks of $\mathbf{Y}_{\mathrm{grid}}(s)$; $\boldsymbol{B}_{\mathrm{red}}$ is the network-side admittance matrix after removing the sources within the network; $\boldsymbol{B}_{nn}$, $\boldsymbol{B}_{nm}$, $\boldsymbol{B}_{mn}$ and $\boldsymbol{B}_{mm}$ are the four blocks of $\boldsymbol{B}_{\mathrm{red}}$; s is the Laplace transform operator; σ is the ratio of the line resistance to line inductance; ω_0 is the synchronous speed.

Based on the closed-loop dynamics of the systems, the closed-loop characteristic equation of the GFMMSs can be expressed as

$$0 = \det\left[(\boldsymbol{S}_{\mathrm{B}}\otimes I_2)\,\mathbf{Y}_{\mathrm{C}}^{N}(s)\mathbf{Y}_{\mathrm{grid}}^{-1}(s) + I_2\right] \tag{7}$$

B. Equivalent Homogeneous System of GFMMSs and GFM Weakest Subsystem

Since the inherent heterogeneity prevents the subsequent decoupling, we construct an equivalent homogeneous system based on Eq. (7) to derive its weakest subsystem. This transformation not only enables the analysis but also reduces computational complexity.

First, by applying matrix perturbation theory [11], an equivalent homogeneous system $\bar{\mathbf{Y}}_{\mathrm{sys}}(s)$ is constructed, whose stability characteristics closely match those of the original system $\mathbf{Y}_{\mathrm{sys}}(s)$, thereby providing an accurate approximation of its overall stability behavior, and can be expressed as

$$\bar{\mathbf{Y}}_{\mathrm{sys}}(s) = \boldsymbol{I}_n\otimes\mathbf{Y}_{\mathrm{eq}}(s) + \boldsymbol{B}_{\mathrm{eq}}\otimes\boldsymbol{\gamma}(s) \tag{8}$$

$$\mathbf{Y}_{\mathrm{eq}}(s) = \sum_{i=1}^{n} p_{1i}\,\mathbf{Y}_{\mathrm{C},i}(s) \tag{9}$$

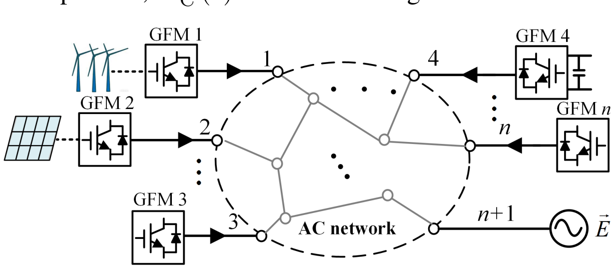

Fig. 1. GFM multi-converter systems.

979-8-3315-8138-1

$$\boldsymbol{B}_{\text{eq}} = \boldsymbol{S}_{\text{B}}^{-1/2}\boldsymbol{B}_{\text{red}}\boldsymbol{S}_{\text{B}}^{-1/2} \tag{10}$$

$$p_{1i} = \frac{\partial \lambda_1}{\partial \left(\boldsymbol{B}_{\text{eq}}\right)_{ii}} = v_{1i}u_{1i} = u_{1i}^2 = v_{1i}^2 \tag{11}$$

where, $\mathbf{Y}_{\text{eq}}(s)$ represents the equivalent admittance model of the homogeneous converters, obtained by aggregating the admittance models $\mathbf{Y}_{\text{C},i}(s)$ of n GFM converters; $\boldsymbol{I}_n$ denotes an $n \times n$ identity matrix; $\boldsymbol{B}_{\text{eq}}$ is the extended admittance matrix; p_{1i} denotes the participation factor of the i-th converter node in the systems; λ_1 is largest eigenvalue of $\boldsymbol{B}_{\text{eq}}$; $(\boldsymbol{B}_{\text{eq}})_{ii}$ denotes the i-th diagonal element; u_{1i} and v_{1i} denote the i-th elements of the left and right eigenvectors $\boldsymbol{u}_1^{\text{T}}$ and $\boldsymbol{v}_1$ corresponding to λ_1.

From Eq. (11), it can be seen that the systems contain n participation factors, each corresponding to one GFM converter node in the GFMMSs.

At this point, based on Eq. (8), an equivalent homogeneous system whose stability characteristics closely match those of the original system has been constructed. The dominant stability trajectory of the original system's admittance $\mathbf{Y}_{\text{sys}}(s)$ can be equivalently represented by that of the homogeneous system $\bar{\mathbf{Y}}_{\text{sys}}(s)$. To quantify the fidelity of this approximation, we adopt the spectral norm (induced 2-norm) as the error metric. Numerical verification on the benchmark system reveals a relative error $\|\mathbf{Y}_{\text{sys}} - \overline{\mathbf{Y}}_{\text{sys}}\|_2 / \|\mathbf{Y}_{\text{sys}}\|_2$ on the order of 10^{-2}. Crucially, however, the deviation in dominant poles between the two models is less than 10^{-3}. This confirms that the approximation error is sufficiently small for LFO analysis.

By performing a similarity transformation using the eigenvector matrix $\boldsymbol{U}$ of $\boldsymbol{B}_{\text{eq}}$ (specifically, left-multiplying by $\boldsymbol{U}^{-1} \otimes \boldsymbol{I}_2$ and right-multiplying by $\boldsymbol{U} \otimes \boldsymbol{I}_2$), the system characteristic equation is decoupled as

$$\begin{aligned} 0 &= \det\left(\boldsymbol{I}_n \otimes \mathbf{Y}_{\text{eq}}(s) + \boldsymbol{B}_{\text{eq}} \otimes \boldsymbol{\gamma}(s)\right) \\ &= \prod_{i=1}^{n} \det\left(\mathbf{Y}_{\text{eq}}(s) + \lambda_i \otimes \boldsymbol{\gamma}(s)\right) \end{aligned} \tag{12}$$

Since the extended admittance matrix $\boldsymbol{B}_{\text{eq}}$ is positive definite, its eigenvalue decomposition yields n single-converter subsystems. λ_i denotes the i-th eigenvalue of $\boldsymbol{B}_{\text{eq}}$ and the eigenvalues satisfy $\lambda_1 \geq \lambda_2 \geq \cdots \geq \lambda_n > 0$.

Definition II.1. The subsystem associated with the largest eigenvalue λ_1 dominates the stability of the GFMMSs and is defined as the weakest subsystem. Its closed-loop characteristic equation can be expressed as

$$\det\left(\mathbf{Y}_{\text{eq}}(s)\boldsymbol{\gamma}^{-1}(s) + \lambda_1 I_2\right) = 0 \tag{13}$$

The original GFMMSs can be mapped to its weakest subsystem, as shown in Fig. 2.

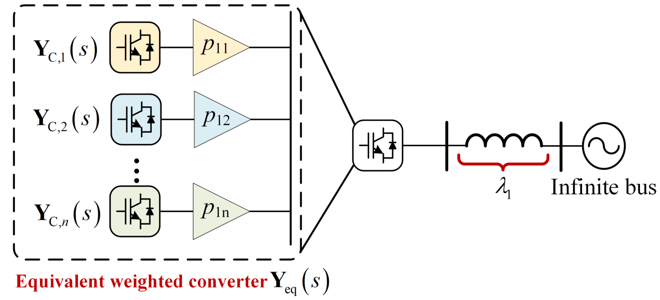

Fig. 2. GFM weakest subsystem of the GFMMSs.

III. LFO Mitigation Strategy for the GFMMSs

In this section, we first introduce and prove the distribution characteristics of the participation factors. Based on this property, the OCNs are defined to enable targeted mitigation of LFOs. Finally, a complete LFO mitigation procedure for the GFMMSs is established.

A. Distribution Characteristic of the Participation Factors

To support the identification of OCNs in GFMMSs, a fundamental property is established as follows.

Property 1 (Distribution characteristic of the participation factors)**.** *In the extended admittance matrix $\boldsymbol{B}_{\text{eq}}$, the participation factors p_{1i} associated with the largest eigenvalue λ_1 exhibit a distinctive distribution characteristic. Specifically, the participation factor p_{1i} attains significantly large values at only a few nodes while approaching zero at most others, forming a "many small and few large" distribution pattern.*

Proof. From the definition of the extended admittance matrix $\boldsymbol{B}_{\text{eq}}$, the Rayleigh quotient $R(x)$ can be expressed as follows

$$R(x) \approx \sum w_{ij}\left(\frac{x_i}{\sqrt{s_i}} - \frac{x_j}{\sqrt{s_j}}\right)^2 \tag{14}$$

where i and j denote the indices of internal nodes; x_i and x_j are the ith and jth components of the eigenvector x, respectively; w_{ij} represents the admittance weighting of the branch between nodes i and j; s_i denotes the converter capacity corresponding to node i.

Under the normalization constraint $\boldsymbol{x}^{\text{T}}\boldsymbol{x} = 1$, the Rayleigh–Ritz theorem implies that the maximum value of $R(x)$ corresponds to the largest eigenvalue λ_1 of the extended admittance matrix $\boldsymbol{B}_{\text{eq}}$, with $\boldsymbol{x} = \boldsymbol{v}_1$ being the associated eigenvector. To maximize the value of $R(x)$ in Eq. (14), the eigenvector $\boldsymbol{v}_1$ must amplify the difference terms between adjacent nodes, i.e., $\left|x_i/\sqrt{s_i} - x_j/\sqrt{s_j}\right|$, implying that the normalized eigenvector components x_i and x_j of neighboring nodes exhibit pronounced numerical differences. Physically, this is analogous to maximizing the potential energy in a spring network, where the interaction energy is concentrated along the most critical topological paths.

Such amplification naturally induces a localized eigenvector structure: only a few components of $\boldsymbol{v}_1$ reach relatively large values, whereas most others approach zero. According to Eq. (11), the participation factor p_{1i} inherits this localization behavior, yielding large values at only a few nodes (i.e., the OCNs), while most other nodes contribute negligibly. □

Remark 1. *Property 1 implies that GFMMS stability is dominated by a few converters located at OCNs, while the remaining converters have negligible influence on the dominant mode.*

979-8-3315-8138-1

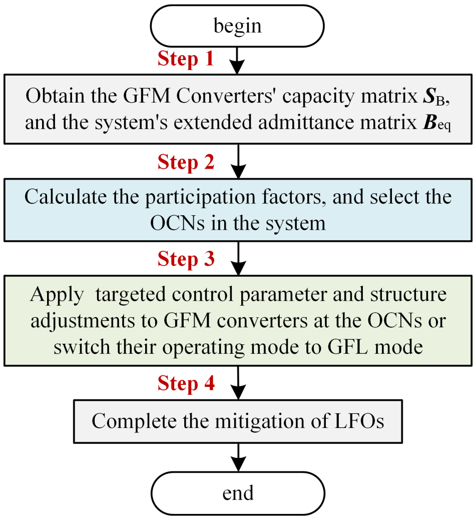

Fig. 3. Flowchart of the OCNs identification and optimization.

B. LFO Mitigation Strategy for the GFMMSs

With the property in Section III-A, the participation factors are employed to quantify the influence of each converter node on the stability of the GFMMSs, leading to the following definition of the OCNs.

Definition III.1. In the GFMMSs, the converter nodes with larger participation factors are defined as the OCNs.

Therefore, LFOs in GFMMSs should be mitigated by targeting the GFM converters located at the OCNs, achieving minimal control intervention. The mitigation strategies can be implemented from two aspects: targeted control parameter and structure adjustments, and control mode switching, as described below.

1) Targeted Control Parameter and Structure Adjustments: If the control parameters and structures of the converters are known, targeted control parameter and structure adjustments can be applied to the GFM converters. Such adjustments include parameter tuning and the introduction of additional control loops. Since LFOs in GFM converters mainly originate from the negative damping effect of the outer voltage control loop, any measure that increases positive damping will enhance converter stability and mitigate oscillations. This principle is applicable to both matching control and VSG control. For instance, in VSG control, increasing the damping coefficient or introducing an additional control loop can effectively improve damping and mitigate LFOs.

2) Control Mode Switching: If the control modes of the GFM converters are adjustable, the GFM converters at the OCNs can be switched to GFL mode. In a strong grid, GFM converters may also cause LFOs since they behave as voltage sources. When multiple voltage source devices with different dynamic characteristics are located electrically close to each other, the system naturally tends to instability. In contrast, GFL converters typically behave as current sources in the low-frequency range. Hence, switching the GFM converters at the OCNs to GFL mode can effectively avoid LFOs caused by interactions among multiple voltage sources.

The LFO mitigation process of the GFMMSs is shown in Fig. 3.

1) Obtain the GFM converters' capacity matrix $\boldsymbol{S}_{\mathrm{B}}$ and the system's extended admittance matrix $\boldsymbol{B}_{\mathrm{eq}}$.
2) Calculate the participation factors, and select the OCNs in the system.
3) Apply targeted control parameter and structure adjustments to GFM converters at the OCNs or switch their operating mode to GFL mode.
4) Complete the mitigation of LFOs.

It is worth noting that, unlike traditional modal analysis that requires detailed white-box dynamic models of all converters and an eigenvalue decomposition of the full closed-loop state matrix of order N, with a typical computational complexity of $O(N^3)$ (N denotes the order of the full closed-loop state-space model of the GFMMSs), the proposed approach identifies the OCNs using only the participation factors derived from $\boldsymbol{B}_{\mathrm{eq}}$. Since dimension of $\boldsymbol{B}_{\mathrm{eq}}$ is n (with $n \ll N$), only the largest eigenpair of an $n \times n$ matrix is required, resulting in a significantly lower computational complexity of $O(n^2)$. This makes the strategy highly practical and well suited for the rapid identification of critical nodes in GFMMSs. It is worth noting that while this work focuses on grid-connected operation with an infinite bus, the proposed method is also applicable to islanded systems.

IV. Simulation Results

To verify the effectiveness of the proposed LFO mitigation strategy, a simulation model of the IEEE 39-bus interconnected system was established in MATLAB/Simulink. Nodes 30–35 and 37–39 are equipped with GFM converters, hereafter denoted GFM1–GFM9 in ascending bus order. Node 36 is modeled as an infinite bus, and the remaining nodes are passive intermediate nodes.

The participation factors of the 9 GFM converter nodes, obtained from the largest eigenvalue of the extended admittance matrix $\boldsymbol{B}_{\mathrm{eq}}$, are 0.00, 0.00, 0.00, 0.64, 0.33, 0.03, 0.00, 0.00, and 0.00, as illustrated in Fig. 5. It can be observed that the participation factors exhibit a distinctive distribution characteristic: the GFM converters at nodes 4 and 5 have the highest participation values of 0.64 and 0.33, respectively, while those of the other nodes are approximately 0.00. Therefore, GFM converter nodes 4 and 5 are identified as the OCNs, which indicates that GFM4 and GFM5 dominate the stability of the IEEE 39-bus interconnected system. As a result, additional control loops are introduced at the GFM converters at nodes 4 and 5, or GFM converters at nodes 4 and 5 are switched to GFL mode. For comparison, the GFM converters at nodes 2 and 9 are selected for simulation.

A. Example 1: Introduction of Additional Control Loops

Time-domain simulations under a voltage dip are conducted, as shown in Fig. 4(a)-(c). The baseline system (Fig. 4(a)) exhibits sustained oscillations. As detailed in Table I, introducing virtual impedance to the identified OCNs (GFM 4 and 5) rapidly suppresses these oscillations, effectively stabilizing

979-8-3315-8138-1

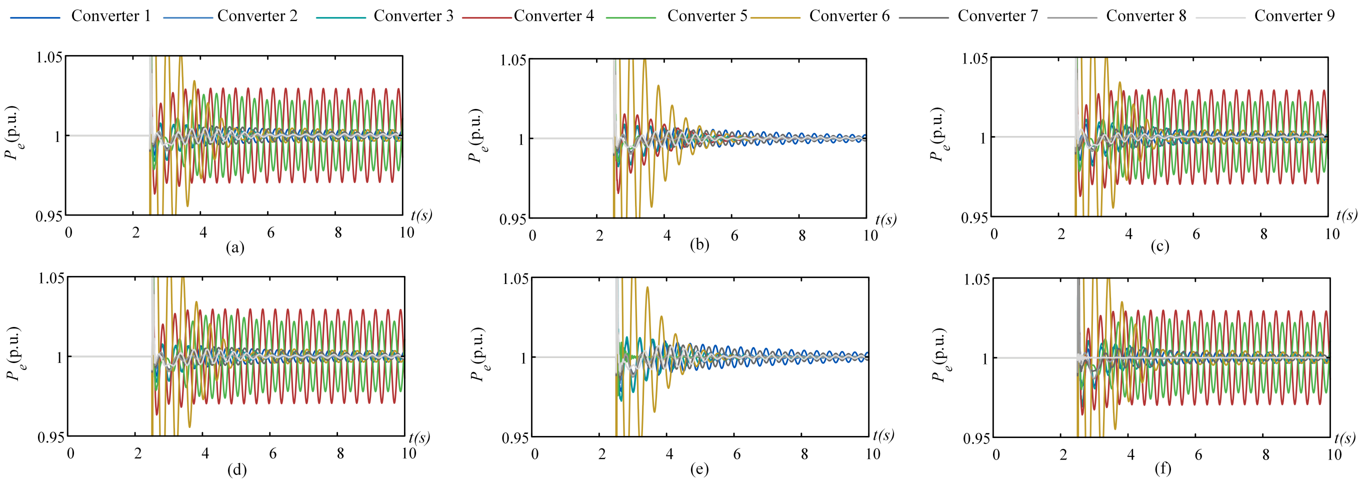

Fig. 4. Active power curves of converters for three cases.

the system. In contrast, applying the same mitigation to non-oscillation critical nodes (Non-OCNs), such as GFM 2 and 9, fails to alter the critical state, as shown in Fig. 4(c). These results confirm that targeting OCNs is crucial for stability enhancement.

B. Example 2: Control Mode Switching

The effectiveness of mode switching is similarly verified, as shown in Fig. 4(d)-(f). The baseline (Fig. 4(d)) shows similar instability. Consistent with Example 1, switching the OCNs (GFM 4 and 5) to GFL mode significantly enhances stability, as evidenced by the quantitative metrics in Table I. Conversely, switching Non-OCNs (GFM 2 and 9) proves ineffective, leaving the system in a critical state (Fig. 4(f)). This comparison further validates that targeted mitigation at OCNs is sufficient to eliminate LFOs with minimal intervention.

TABLE I
COMPARISON OF STABILITY METRICS UNDER DIFFERENT STRATEGIES

Scenario	Dominant Poles (λ)	ζ (%)	State
Baseline (No Control)	$-0.001 \pm j16.90$	0.01	Critical
Method I: Additional Damping Control			
OCNs (GFM 4, 5)	$-0.209 \pm j16.71$	1.25	Stable
Non-OCNs (GFM 2, 9)	$-0.002 \pm j16.90$	0.01	Critical
Method II: Mode Switching to GFL			
OCNs (GFM 4, 5)	$-0.205 \pm j16.72$	1.23	Stable
Non-OCNs (GFM 2, 9)	$-0.001 \pm j16.90$	0.01	Critical

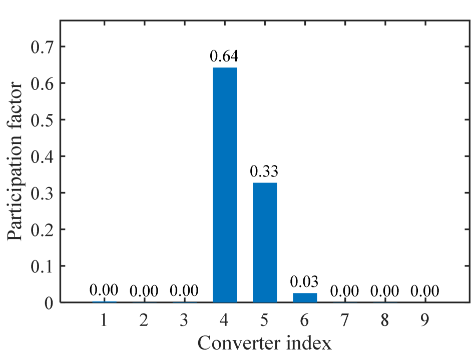

Fig. 5. The participation factors of the 9 GFM converter nodes in the IEEE 39-bus interconnected system.

V. CONCLUSIONS

GFM converters play a crucial role in supporting modern power systems, and the stability issues of multi-converter operations are becoming increasingly prominent. This paper proposes an LFO mitigation strategy based on participation factors of the extended admittance matrix. The proposed strategy significantly mitigates LFOs in GFMMSs while featuring a substantially lower computational complexity.

Future research could further investigate the stability of GFMMSs under large disturbances.

REFERENCES

[1] X. Wang, M. G. Taul, H. Wu, Y. Liao, F. Blaabjerg, and L. Harnefors, "Grid-synchronization stability of converter-based resources—an overview," *IEEE Open Journal of Industry Applications*, vol. 1, pp. 115–134, 2020.

[2] L. Fan and Z. Miao, "Wind in weak grids: 4 hz or 30 hz oscillations?" *IEEE Transactions on Power Systems*, vol. 33, no. 5, pp. 5803–5804, 2018.

[3] Y. Gu and T. C. Green, "Power system stability with a high penetration of inverter-based resources," *Proceedings of the IEEE*, vol. 111, no. 7, pp. 832–853, 2022.

[4] B. B. Johnson, S. V. Dhople, A. O. Hamadeh, and P. T. Krein, "Synchronization of parallel single-phase inverters with virtual oscillator control," *IEEE Transactions on Power Electronics*, vol. 29, no. 11, pp. 6124–6138, 2013.

[5] C. Yang, L. Huang, H. Xin, and P. Ju, "Placing grid-forming converters to enhance small signal stability of pll-integrated power systems," *IEEE Transactions on Power Systems*, vol. 36, no. 4, pp. 3563–3573, 2020.

[6] J. Tan, S. Dong, and A. Hoke, "Lessons learned from real-world oscillation events," in *IEEE PES General Meeting, Orlando, FL, USA*, 2023, pp. 16–20.

[7] Y. Tian, X. Xu, Y. Wang, Z. Li, Z. Zhang, and Y. Gao, "Full-state feedback power decoupling control for grid forming converter with improved stability and inertia response," *IEEE Transactions on Power Electronics*, 2024.

[8] X. Wang, Y. W. Li, F. Blaabjerg, and P. C. Loh, "Virtual-impedance-based control for voltage-source and current-source converters," *IEEE Transactions on Power Electronics*, vol. 30, no. 12, pp. 7019–7037, 2014.

[9] J. Lin, S. Liu, and G. Wang, "Stability analysis and control parameter optimization of multi-vsg parallel grid-connected system," *Electric Power Systems Research*, vol. 221, p. 109478, 2023.

[10] F. Chen, X. Wang, L. Harnefors, S. Z. Khong, J. Kukkola, M. Routimo, L. Zhao, D. Wang, H. Sandberg, K. C. Sou *et al.*, "Assessment, cause localization, and mitigation for small-signal stability risks in multi-parallel grid-forming converter systems," *IEEE Transactions on Smart Grid*, 2025.

[11] G. W. Stewart, "Stochastic perturbation theory," *SIAM review*, vol. 32, no. 4, pp. 579–610, 1990.

979-8-3315-8138-1